other factors that might influence DNA conductivity. For example, if vibrational modes of the molecules participate in the conduction mechanism, a certain length of the molecule may simply be required to allow for those collective effects, like solitons, to build up and to mediate electron transport. This would imply that restrictions of the degree of freedom of the DNA molecules such as through adsorption to a surface for example, could affect electrical conduction. There are probably a range of other issues that need to be considered to understand the details of the conduction mechanism on a molecular scale, but they do not affect our finding that DNA molecules, under the conditions described here, are electrical conductors. Further carefully designed experiments are now needed to explore the factors influencing DNA conductivity. Measurements of the temperature dependence of DNA resistivity, as well as the characterization of the electrical noise, should help to determine how DNA transports charges.

The detailed understanding of the conduction mechanism remains a challenge and, once achieved, should undoubtedly provide a better insight into the biological, chemical and physical properties of DNA molecules. The work reported here suggests that DNA molecules should be considered, among other candidates, as potential one-dimensional quantum wires for mesoscopic devices. □

1. Dandliker, P. J., Holmlin, R. E. & Barton, J. K. Oxidative thymine dimer repair in the DNA helix. *Science* **257**, 1465–1468 (1997).
2. Arkin, M. R. *et al.* Rates of DNA-mediated electron transfer between metallointercalators. *Science* **273**, 475–480 (1996).
3. Lewis, F. D. *et al.* Distance-dependent electron transfer in DNA hairpins. *Science* **277**, 673–676 (1997).
4. Beratan, D. N., Priyadarshy, S. & Risser, S. M. DNA: insulator or wire? *Chem. Biol.* **4**, 3–8 (1997).
5. Fink, H.-W., Stocker, W. & Schmid, H. Holography with low energy electrons. *Phys. Rev. Lett.* **65**, 1204–1206 (1990).
6. Schmid, H. & Fink, H.-W. Carbon nanotubes are coherent electron sources. *Appl. Phys. Lett.* **70**, 2679–2680 (1997).
7. Fink, H.-W., Schmid, H., Ermantraut, E. & Schulz, T. Electron holography of individual DNA molecules. *J. Opt. Soc. Am. A* **14**, 2168–2172 (1997).
8. Austin, R. H. Stretch genes. *Phys. Today* 32–38 (February 1997).

Glacial–interglacial changes in ocean surface conditions in the Southern Hemisphere

F. Vimeux*, V. Masson*, J. Jouzel*, M. Stievenard* & J. R. Petit†

* Laboratoire des Sciences du Climat et de l'Environnement (UMR CEA/CNRS 1572), L'Orme des Merisiers, Bâtiment 709, CEA Saclay, 91191 Gif-sur-Yvette cédex, France
† Laboratoire de Glaciologie et de Géophysique de l'Environnement (CNRS), 54 rue Molière, Domaine Universitaire, BP 96, 38402 St-Martin d'Héres cédex, France

....

The stable-isotope signatures of oxygen and hydrogen in the water of preserved ice and snow are both widely used to infer local temperatures of past environments. A derived quantity based on these two signatures, the 'deuterium excess'[1], provides additional palaeoclimatic information[2-4], as this parameter depends on the meteorological and oceanic characteristics of the water's source-regions (in particular, their temperature[2,3] and relative humidity[4]). Published studies mainly focus on records from the past 40,000 years. Here we present a deuterium-excess history obtained from ice cores from Vostok, East Antarctica, spanning the full glacial–interglacial cycle of the past 150,000 years. The deuterium-excess record shows a strong anticorrelation with the Earth's orbital obliquity (~41,000-year periodicity), and values are markedly higher during the cold stage 5d (following the last interglacial) than during the other cold stages. We interpret the relationship with obliquity as resulting from changes in the latitudinal insolation gradient affecting ocean surface conditions and, thus, the delivery of moisture to the polar region. We argue that the high 5d values, relative to other cold stages, are driven by relatively less moisture delivered from high latitudes, and more from low latitudes. The deuterium-excess in Antarctic precipitation thus provides long-term, spatially integrated information on ocean surface conditions and ocean/atmosphere circulations in the Southern Hemisphere.

The deuterium excess, d, (hereafter the excess) is defined as the deviation from the meteoric water line[5]: $d = \delta D - 8\delta^{18}O$ (see Fig. 1
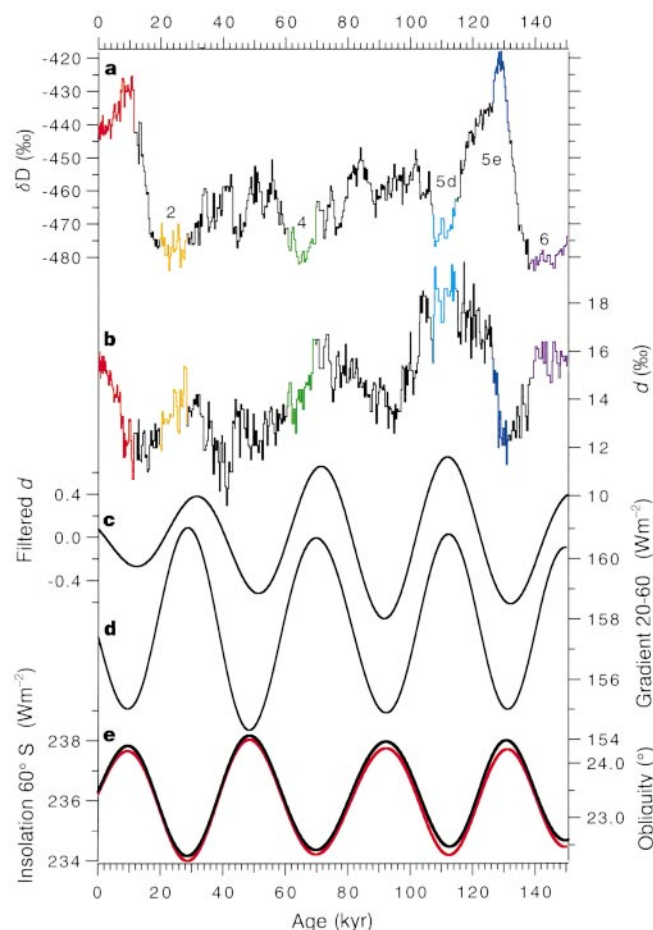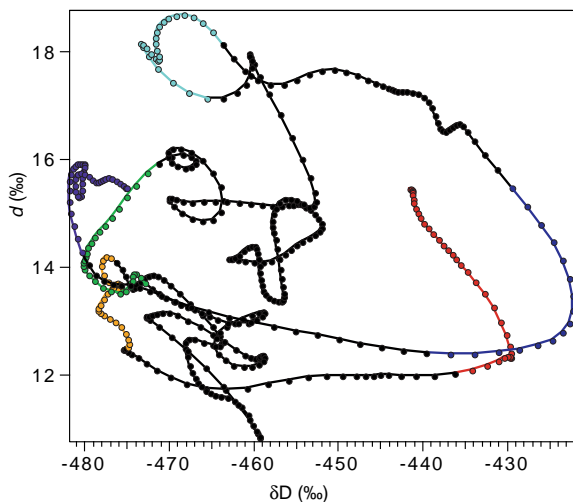

Figure 1 Time series of δD, deuterium excess, obliquity and insolation. **a**, δD; **b**, deuterium excess, d. Measurements were performed along a shallow core from the surface to 138 m (BH8, drilled in 1996) and along deep core 3G from 138 to 2,083 m, with different sampling resolutions (50 cm between 0 and 138 m; 5 m down to 1413 m, 2 m below this[10]). Experimental accuracy for deuterium excess is ±0.7‰ (±0.5‰ for δD and ±0.05‰ for δ^{18}O) down to 1,413 m and ±1.3‰ below this (δ^{18}O measurements were performed with a dual mass spectrometer with a precision of ±0.1‰). Data are presented at a 5-m depth resolution representing a temporal resolution of 200 to 500 years. We use a modified version of the extended glaciological timescale, the accuracy of which is estimated to be ±6 kyr (ref. 10). **c**, Gaussian-filtered deuterium excess in the obliquity band (0.025± 0.005 kyr^{-1}). **d**, Difference between mean annual insolation at 20° S and 60° S. **e**, Mean annual insolation at 60° S (black line), and obliquity[14] (red line). (Here $\delta D = ([(D/H)_{sample}/(D/H)_{vsmow}] - 1) \times 10^3$; $\delta^{18}O = ([(^{18}O/^{16}O)_{sample}/(^{18}O/^{16}O)_{vsmow}] - 1) \times 10^3$.)

legend for nomenclature). The excess mainly reflects the kinetic fractionation occurring during non-equilibrium processes (evaporation above the ocean[6] surface and snow formation[7]) due to the difference in diffusivity between heavy and light molecules. As shown by simple models based on the closure equation[3,6], the excess in the vapour above the ocean surface increases when the ocean surface temperature increases (+0.35‰ per °C) and decreases when relative humidity increases (−0.43‰ per %). Simple models[3,8] have also shown that the initial excess value reflecting the oceanic source information is, at least partly, preserved all over the air-mass trajectory towards polar regions. Recent results obtained with a more complex atmospheric general circulation model (AGCM) calibrated with isotope tracer diagnostics support the idea that polar deuterium-excess values contain information on meteorological conditions at distant evaporative sources[9].

The Vostok ice-core deuterium-excess profile is shown in Fig. 1 along with δD (ref. 10), a proxy of local past temperatures changes (see ref. 11 for a recent review). This record covers a full climatic cycle back to 150 kyr before present and considerably extends the 40-kyr Antarctic continuous record from Dome C (ref. 4; except for this site and for limited discontinuous Vostok data[10], most studies of deuterium excess in Antarctica have focused on surface snow). Large variations are found in this record, from ~10‰ to 20‰. For the first 40 kyr, we note similar excess changes at Vostok and Dome C. In particular, for both records, the excess is 4−5‰ lower over the deglaciation than for the youngest part of the Holocene, indicating that glacial–interglacial fluctuations in Vostok excess represent at least a synoptic-scale pattern. We note a general anti-correlation between d and δD. However, Fig. 2, in which d is plotted as a function of δD, illustrates that the excess contains additional information compared to the deuterium profile. This is confirmed by a principal-component analysis performed on the two isotopes which provides (as second component) a combination similar to the excess profile.

During the two interglacial periods characterized by high δD values (Holocene in red and Eemian in dark blue; Figs 1 and 2) the excess increases with time. During transitions (characterized by large δD changes), two distinct types of excess behaviour appear; glacial inception with high excess values and deglaciations with low excess values. During glacial periods (low δD values), various excess levels can be present for a given temperature. In particular, stage 5d is characterized by the highest excess values (~19.5‰), whereas stages 2, 4 and 6 have lower excess values (~15‰). Before

interpreting this obvious feature, we examine the spectral properties of the excess signal.

Various spectral methods have been used, and we have tested that the spectral properties are robust with respect to the empirically based definition of the excess by replacing 8.0 by any value between 7.0 and 9.0 (note that, in our record, the δD−δ^{18}O slope is 7.85). We conclude that only the obliquity (41-kyr periodicity) is strongly significant for the excess, and that it differs from the local δD temperature record for which both obliquity and precession (23-kyr) are significant (Fig. 3 shows only results from the multi-taper method[12]). A cross-spectral analysis of coherence and phase (using the Blackman–Tukey method[13]) between the excess and the obliquity points out their strong anticorrelation over the past 150 kyr. This is illustrated by comparing the excess values filtered in the 40-kyr band with the obliquity: the highest (lowest) values of deuterium excess are in phase with the lowest (highest) values of obliquity (Fig. 1). This orbital parameter strongly modulates the annual mean insolation[14], in particular at high latitudes (Fig. 1) and we now examine how annual insolation changes could influence the deuterium excess of Antarctic snow.

First, Vostok local temperatures are partly influenced by the obliquity (as indicated by δD) and we could therefore think of the 40-kyr excess modulation as being due to local post-deposition effects such as those related to sublimation and depth-hoar formation (ice crystals formed by sublimation within snow, but beneath the snow surface) which, under certain conditions, may induce additional kinetic fractionation[15]. However, due to the extremely low temperatures in Vostok, this possibility can probably be discarded. Second, a recent study with an AGCM coupled with a slab ocean model has shown the effects of obliquity fluctuations on high-latitude climate due to the response of sea-ice cover. Increased obliquity (increased annual insolation at 60° S) and therefore reduced sea-ice cover[16] induces a larger relative contribution of local cold moisture sources, resulting in low excess values, and vice
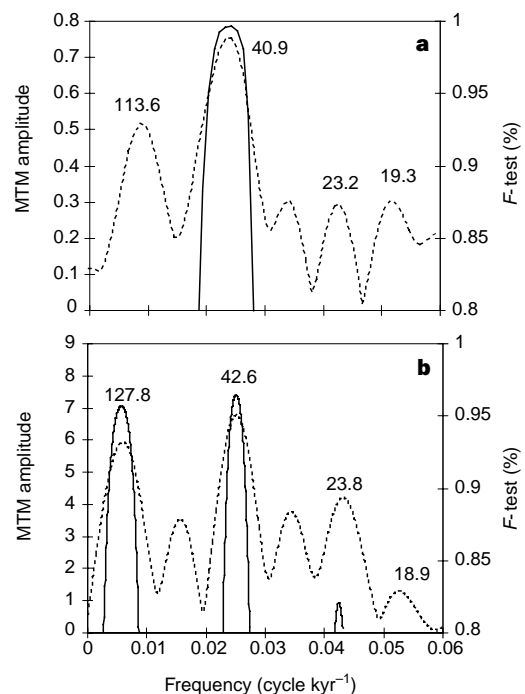
Figure 3 Harmonic analysis of the deuterium excess (**a**) and δD (**b**) interpolated at 0.5-kyr intervals. The analysis used the multi-taper method (MTM); the bandwidth parameter, NΩ, is 4 and the number of tapers is 6 (see ref. 12 for details). This non-parametric method provides high-frequency resolution and has the advantage of providing a statistical test (solid line) for the validity of the amplitude (dashed line) and the location of each peak. Calculations have been performed with the Analyseries software[30].

Figure 2 Deuterium excess versus δD (with smoothing over a 4,500-year running period). The colour represents the different stages as defined in Fig. 1: Holocene (red), Last Glacial Maximum (orange), stage 4 (green), stage 5d (light blue), last interglacial (dark blue) and previous glacial period (purple).

Table 1 Comparison of Vostok coldest stages 2, 4, 5d and 6

	Stage 2	Stage 4	Stage 5d	Stage 6	References
Vostok temperature (°C)*†	−6	−6	−5	−7	Ref. 10
Vostok deuterium excess (‰)*	14.5	15	18.5	15.5	This study
Vostok marine sodium (ng g^{-1})*	110	85	50	80	Ref. 22
Vostok dust (10^{-9} cm^3 g^{-1})*	690	510	4	404	Ref. 24
Sea surface temperature (°C) from MD 85668, 0° 01′ S, 46° 02′ E*†	−1.6	−0.7	+0.3	−0.4	Ref. 19
Sea surface temperature (°C) from MD 84 527, 43° 49′ S, 51°19′ E*†	−4.0	−4.2	−4.1	−3.8	Ref. 29

* Averaged values during the coldest parts of stages 2, 4, 5d and 6.
† Temperatures deviations from their Holocene values.

versa. Although a significant influence of high-latitude oceans south of the polar front on central Antarctic precipitation is supported by AGCM simulations of present-day moisture sources, this contribution is too low (~15%) to explain by itself the 40-kyr modulation[17].

Third, annual insolations are in phase with obliquity south of ~45° S and in antiphase from there to the Equator. Thus obliquity fluctuations significantly modulate the difference between annual insolations at low and high latitudes (~4% for the difference 20° S–60° S, Fig. 1) and have effects on both atmospheric and ocean circulations (moisture and heat transport). A minimum latitudinal insolation gradient weakens the atmospheric meridional circulation and reduces the contribution of low-latitude moisture to Antarctic precipitation. In parallel, less oceanic heat transport from low to high latitudes results in lower sea surface temperature (SST) at high latitudes. Both effects contribute to a colder origin for the precipitation and therefore excess values are lower when the insolation gradient is weak, that is, when the obliquity is large. This change in source temperatures also affects the Antarctic snow isotopic content: if relative humidity is kept constant, a colder source implies an increase of δD and δ^{18}O and vice versa. Indeed this may explain the generally observed anticorrelation between d and δD. Part of the 40-kyr modulation in the Vostok isotopic record may result from an associated shift of the polar front which is itself reflected in the deuterium excess (by inducing a parallel shift in the source areas).

Although the influence of changes in relative humidity cannot be discarded[4], we favour the SST interpretation for two reasons. First, simple isotopic models show that the imprint of the source temperature on Antarctic snow deuterium excess increases inland while the imprint of the source relative humidity[8] decreases. Second, we have analysed the modern and glacial climates simulated by various AGCMs within the Paleoclimate Modeling Intercomparison Project[18]. All models show only weak relative humidity changes (typically 1%) above southern oceans north of the polar front.

The changes in respective contributions of low- and high-latitude moisture also provide a plausible explanation for the extremely high excess level during cold stage 5d compared with the other cold periods (stages 2, 4, 6). The high latitudes are characterized by similarly cold temperatures during all these stages (Table 1), but, during glacial inception, the southern tropics are warmer than during stages 2, 4 and 6 as generally shown by available ocean cores[19–21] covering these periods. Indeed, the high excess level implies a strong contribution of moisture from the warm ocean and suggests that, during glacial inception, low-latitude evaporation was maintained at its interglacial level.

Moreover, the Vostok marine sodium profile[22] shows much lower concentrations during stage 5d than during stages 2, 4 and 6 (Table 1), probably associated with a decreased atmospheric transport from production regions (high latitudes) to the ice cap[23]. Dust concentrations in the Vostok ice are also different in stage 5d (no dust) than in the other glacial periods[24]. The absence of dust peaks during stage 5d may be also due to a weaker atmospheric circulation[23,24] over the dust sources (mainly South America[25]).

The combined information from marine sodium and dust suggests a weakened atmospheric circulation at high latitudes[24] during stage 5d and therefore less atmospheric transport of high latitude moisture. Thus, two phenomena are different at stage 5d

compared with stages 2, 4 and 6: warmer SST in the equatorial region, possibly maintaining local evaporation, and less atmospheric transport from the high latitudes as indicated by dust and marine sodium records. As a result, the relative contribution of low latitudes to Vostok precipitation would be higher during stage 5d than during other Vostok cold stages, explaining higher values of deuterium excess.

The study of the last climatic cycle in Vostok points out the importance of the moisture origin, and the relative contribution of low and high latitudes, in controlling the excess values. Therefore, the deuterium excess provides integrated, and thus unique, information on oceanic conditions and their past fluctuations, complementing relatively scarce southern deep-sea core data. The use of isotopic AGCMs should help to quantify better the changes in the deuterium excess and the link of relevant oceanic surface parameters with obliquity. Here, using the deuterium excess, we have pointed out the effect of the insolation gradient on the relative contribution of low and high latitudes to Antarctic precipitation (this relative contribution is inaccessible by other means). Indeed, changes in deuterium excess at Vostok also provide an indirect measure of southern latitudinal moisture transport above the ocean. The importance of this latitudinal moisture transport on thermohaline oceanic circulation is now fully recognized for the North Atlantic (see ref. 26 and references therein). This should also hold true for the Southern Ocean. In turn, obtaining information on latitudinal moisture transport may help the understanding of the role of the ocean in linking the climates of the Southern and Northern hemispheres[27].

The deuterium excess at Vostok also suggests that oceanic conditions during glacial stage 5d were more similar to an interglacial than to other glacial stages (2, 4, 6); this indicates a significant difference in the hydrological cycle between a cold stage just following an interglacial peak (5e) and a full glacial cold stage. Preliminary results[10] seem to indicate a similar situation for the previous glacial inception (stage 7). The possibility now offered of obtaining a continuous profile of deuterium excess over four climatic cycles in Vostok[28] should allow further investigation of this difference in hydrological cycle; it should also allow further study of the link between deuterium excess, insolation, and surface-condition changes. □

1. Dansgaard, W. Stable isotopes in precipitation. *Tellus* **16**, 436–447 (1964).
2. Dansgaard, W., White, J. W. & Johnsen, S. J. The abrupt termination of the Younger Dryas climate event. *Nature* **339**, 532–534 (1989).
3. Johnsen, S. J., Dansgaard, W. & White, J. W. C. The origin of Arctic precipitation under present and glacial conditions. *Tellus B* **41**, 452–468 (1989).
4. Jouzel, J., Merlivat, L. & Lorius, C. Deuterium excess in an East Antarctic ice core suggests higher relative humidity at the oceanic surface during the last glacial maximum. *Nature* **299**, 688–691 (1982).
5. Craig, H. Isotopic variations in meteoric waters. *Science* **133**, 1702–1703 (1961).
6. Merlivat, L. & Jouzel, J. Global climatic interpretation of the deuterium-oxygen 18 relationship for precipitation. *J. Geophys. Res.* **84**, 5029–5033 (1979).
7. Jouzel, J. & Merlivat, L. Deuterium and oxygen 18 in precipitation: modelling of the isotopic effects during snow formation. *J. Geophys. Res.* **89**, 11749–11757 (1984).
8. Petit, J. R., White, J. W. C., Young, N. W., Jouzel, J. & Korotkevich, Y. S. Deuterium excess in recent Antarctic snow. *J. Geophys. Res.* **96**, 5113–5122 (1991).
9. Armengaud, A., Koster, R., Jouzel, J. & Ciais, P. Deuterium excess in Greenland snow: Analysis with simple and complex models. *J. Geophys. Res.* **103**, 8947–8953 (1998).
10. Jouzel, J. *et al.* Climatic interpretation of the recently extended Vostok ice records. *Clim. Dyn.* **12**, 513–521 (1996).
11. Jouzel, J. *et al.* Validity of the temperature reconstruction from ice cores. *J. Geophys. Res.* **102**, 26471–26487 (1997).
12. Thomson, D. J. Spectrum estimation and harmonic analysis. *Proc. IEEE* **70**, 1055–1096 (1982).

13. Jenkins, G. M. & Watts, D. G. *Spectral Analysis and its Applications* (Holden-Day, San Francisco, 1968).
14. Berger, A. L. Long-term variations of daily insolation and quaternary climatic change. *J. Atmos. Sci.* **35**, 2362–2367 (1978).
15. Satake, H. & Kawada, K. The quantitative evaluation of sublimation and the estimation of original hydrogen and oxygen isotope ratios of a firn core at East Queen Maud Land, Antarctica. *Bull. Glacier Res.* **15**, 93–97 (1997).
16. Gallimore, R. G. & Kutzbach, J. E. Snow cover and sea ice sensitivity to generic changes in Earth orbital parameters. *J. Geophys. Res.* **100**, 1103–1120 (1995).
17. Delaygue, G., Masson, V., Jouzel, J., Koster, R. D. & Healy, R. J. The origin of Antarctic precipitation: a modelling approach. *Tellus* (submitted).
18. Joussaume, S. & Taylor, K. E. in *Proc. 1st AMIP Sci. Conf., WCRP* Vol. 92 425–430 (World Climate Research Program, Monterey, CA, 1995).
19. Bard, E., Rostek, F. & Sonzogni, C. Interhemispheric synchrony of the last deglaciation inferred from alkenone palaeothermometry. *Nature* **385**, 707–710 (1997).
20. Schneider, R. R., Müller, P. J. & Ruhland, G. Late Quaternary surface circulation in the east equatorial South Atlantic: Evidence from alkenone sea surface temperatures. *Paleoceanography* **10**, 197–219 (1995).
21. Van Campo, E., Duplessy, J. C., Prell, W. L., Barratt, N. & Sabatier, R. Comparison of terrestrial and marine temperature estimate for the past 135 kyr off South East Africa: a test for GCM simulations of palaeoclimate. *Nature* **348**, 209–212 (1990).
22. Legrand, M. R., Lorius, C., Barkov, N. I. & Petrov, V. N. Vostok (Antarctica) ice core: atmospheric chemistry changes over the last climatic cycle (160000 years). *Atmos. Environ.* **22**, 317–331 (1988).
23. Genthon, C. Simulations of desert dust and sea-salt aerosols in Antarctica with a general circulation model of the atmosphere. *Tellus B* **44**, 371–389 (1992).
24. Petit, J. R. *et al.* Paleoclimatological and chronological implications of the Vostok core dust record. *Nature* **343**, 56–58 (1990).
25. Basile, I. *et al.* Patagonian origin of glacial dust deposited in East Antarctica (Vostok and Dome C) during glacial stages 2, 4 and 6. *Earth Planet. Sci. Lett.* **143**, 573–590 (1997).
26. Stocker, T. S. & Schmittner, A. Influence of CO_2 emission rates on the stability of the thermohaline circulation. *Nature* **388**, 862–865 (1997).
27. Blunier, T. *et al.* Asynchrony of Antarctica and Greenland climate during the last glacial. *Nature* **394**, 739–743 (1998).
28. Petit, J. R. *et al.* Four climate cycles in Vostok ice core. *Nature* **387**, 359–360 (1997).
29. Pichon, J. J. *et al.* Surface water temperature changes in the high latitudes of the southern hemisphere over the last glacial-interglacial cycle. *Paleoceanography* **7**, 289–318 (1992).
30. Paillard, D., Labeyrie, L. & Yiou, P. Macintosh program performs time-series analysis. *Eos* **77**, 379 (1996).

Gravity-driven continental overflow and Archaean tectonics

R. C. Bailey

Geology and Physics Departments, University of Toronto, 60 St George Street, Toronto, Ontario M5S 1A7, Canada

Whether modern tectonic processes differ substantially from those in Archaean times (>2,500 Myr ago) remains controversial. One view[1] is that Archaean tectonic processes were some combination of modern ones, occurring faster or more shallowly because of the larger heat output of the early Earth, but others[2] have proposed that significantly different processes operated. Here I argue that gravitational spreading of Archaean continents would have caused them continuously and pervasively to 'overflow' onto adjacent ocean basins, and that this process would have naturally ceased at the end of the Archaean era. Because modern continental crust is believed to be ductile rather than brittle below a depth corresponding to a temperature of about 350–400 °C (ref. 3), it seems likely that such a ductile zone was universally present within the hotter Archaean continental crust. If the mean geothermal gradient of the continents had exceeded ~25–30 °C km⁻¹, then the resulting ductile zone would have caused continental overflow to occur, and such a process can account for many of the distinctive peculiarities observed in the Archaean geological record. The cessation of continental overflow corresponds naturally to the stabilizing 'cratonization' which marked the end of the Archaean era, with its timing dependent on the evolution of

both the geothermal gradient in the continents and the depth of the ocean basins.

Processes such as tectonic compression and subduction- or plume-related magmatism can thicken continental crust. The amount of such thickening is limited by gravitational collapse[4], which thins and spreads continental crust. Gravitational spreading uses the gravitational energy of overthickened crust to provide the power needed to drive extensional normal faulting in the upper brittle crust, viscous simple shear of the lower ductile crust, and viscous shear in the mantle as mantle flow accommodates isostatic adjustments of the crust. If the crustal ductile channel is sufficiently inviscid, significant upper-crustal topographic relief cannot be maintained in the spreading region, and must be concentrated in a 'front' at the leading edge (or edges) of a spreading plateau, as observed in Tibet today. Such a front can take one of two forms: if the crust into which the front is propagating also possesses a ductile channel, spreading will drive lower-crustal material into this channel and thicken it, 'inflating' the crust in the manner modelled by Bird[5]. Alternatively, and this is the case I analyse here, the adjacent crust may contain no ductile channel: in particular, it may be oceanic crust, which, although being as hot as the advancing felsic material, is not ductile because of its mafic composition. In this case, frontal advance can proceed only if continental material overflows the oceanic crust by thrusting, as shown schematically in Fig. 1.

To assess the degree of crustal overthickening required to drive an overflow front, I estimate here the magnitude of the various energy dissipation terms relative to the available gravitational power. Because viscous shear heating must be quadratic in the overflow front velocity, it must be negligible at the onset of overflow relative to the other components of the energy budget, which must be linear in the overflow front velocity; the threshold for overflow is therefore determined by the balance of these linear terms. As I will show, the threshold is primarily determined by the balance of gravitational input power and normal-fault dissipation; all other terms are much less important. To show the relative importance of these terms, it is convenient to have a specific and simple example in mind; here I evaluate them for the case of a microcontinent of width L and much longer strike length whose brittle upper crust and deep crustal ductile zone are of uniform thicknesses b and h, respectively (Fig. 1). Spreading is assumed to be perpendicular to strike, increasing L with frontal velocity v_f. For simplicity, I assume that the frontal geometry does not change with extension, although the thicknesses b and h must decrease proportionally with the rate of increase of L in order to conserve mass, the former by normal-fault rotation in the brittle crust, and the latter by Couette (simple shear) flow in the ductile zone (implying that the flow velocity tends to zero at the base of the ductile zone). The simplifying assumption that the depth of the brittle–ductile transition is approximately independent of strain rate is reasonable; the strongly thermally activated nature of any reasonable crustal rheology means that the effective viscosity profile
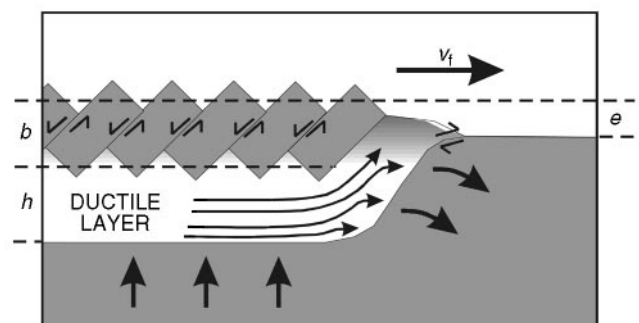

Figure 1 Cross-section perpendicular to strike of a simplified Archaean microcontinent. Symbols are defined in the text.